Corneal Sensory Nerves

Subjects: Physiology | Anatomy & Morphology

Contributor: Laura Frutos-Rincón

The cornea is an avascular connective tissue that is crucial, not only as the primary barrier of the eye but also as a proper transparent refractive structure. Corneal transparency is necessary for vision and is the result of several factors, including its highly organized structure, the physiology of its few cellular components, the absence of blood and lymphatic vessels in healthy conditions, the tightly controlled hydration state, and the lack of myelinated nerves, among others. The cornea is supplied by both sensory and autonomic nerves, being one of the most densely innervated tissues in the body. Corneal innervation is anatomically organized into four levels ranging from the nerve trunks in the corneal stroma to the nerve terminals in the epithelium. Electrophysiological recordings of corneal sensory nerve fibers have revealed the existence of three different functional types of sensory neurons that are classified into mechanonociceptors, polymodal nociceptors and cold thermoreceptors depending on the modality of stimuli by which they are activated. The impulse discharge is conducted by these neurons to the central nervous system, where sensory input is processed to finally evoke a sensation and to regulate ocular protective functions, such as tearing and blinking.

Keywords: cornea ; corneal anatomy ; corneal innervation ; corneal nerves

1. Introduction

The cornea and the conjunctiva constitute the eye tissues exposed to the environment. The cornea is an avascular connective tissue that is crucial, not only as the primary barrier for the eye but also as a powerful refractive structure. As a barrier, the cornea provides structural integrity to the ocular globe and protects its inner components from infectious agents and physical injury or chemical insults. On the other hand, as a refractive structure, it has two key properties: refractive power (for light refraction) and transparency (for light transmission) [1].

The shape of the human cornea is prolate, which creates an aspheric optical system [2]. The human cornea has a refractive index of 1.376 and a dioptric power higher than 40 dioptres, about 2/3 of the total ocular power [3]. It is 540–700 µm thick, being thinner in the center and thicker in the periphery [1]. The human cornea measures about 11 mm vertically and 12 mm horizontally [4] covering the anterior 1/6th of the ocular surface and is organized into 5 layers (**Figure 1**): epithelium, Bowman's layer, stroma, Descemet's membrane, and endothelium. Among species, the cornea keeps the same general structure, with differences in thickness and presence or absence of Bowman's layer.

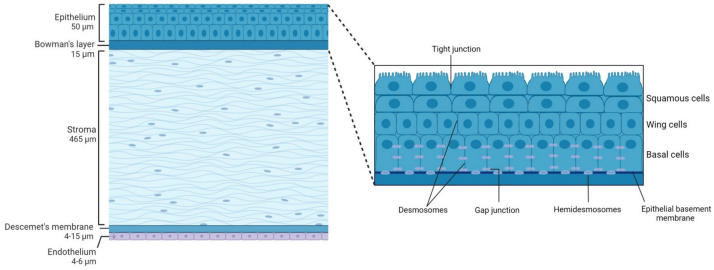

Figure 1. Schematic representation of the corneal structure, showing its five main layers and their thickness. Inset: diagram of the corneal epithelium, showing its different cell layers and details on the different types of cell-cell junctions contributing to corneal epithelium impermeability.

Transparency of all ocular structures is crucial for vision. Transparency of the cornea is the result of many factors including its highly organized anatomical structure, the physiology of its cellular components, the lack of myelination of nerves inside the cornea, its tightly controlled (de)hydration state and the absence of blood and lymphatic vessels, among others. Since vision plays a critical role in obtaining information from the external environment, the cornea also has specific characteristics that ensure its own protection against injury. One of the most important features in this regard is the high sensitivity of the cornea to external insults provided by its extremely rich sensory innervation.

Taking all the corneal characteristics into account, it is clear that the cornea is an ideal model for studying the interactions between corneal nerves and the few cell types present in this quite simple structure. Particularly, the cornea represents a perfect scenario to study neuro–immune interactions for different reasons: the cornea is densely innervated [5][6] with sensory nerves easily accessible for electrophysiological recordings whose functional properties have been described in detail [7][8]; the cornea is fully transparent [9][10], which means that fluorescence data could be gathered at high resolution for both in vivo and ex vivo experiments and finally, the cornea is avascular [11][12], which allows distinguishing the contribution of resident immune cells from that of immune cells migrating from blood vessels.

2. Corneal Structure

2.1. Epithelium

The corneal epithelium composed of a single layer of basal cells and several stratified and non-keratinized cell layers (**Figure 1**, inset), constitutes the first protective ocular barrier against external threats. In humans, it is 50 µm thick, representing around 8% of the total thickness of the cornea [13].

The outermost corneal epithelium constitutes 2–3 layers of squamous cells [2] (**Figure 1**, inset). These cells are flat and polygonal and have apical microvilli which, in turn, are covered by a fine glycocalyx consisting of membrane-associated mucins, including MUC1, MUC4, and MUC16 [14]. These squamous cells maintain tight junctions with their neighbors, which is essential for their function as a barrier to prevent large molecules or microbes from entering the deeper corneal layers. Beneath the superficial layers of squamous cells are the mid-epithelial layers of wing cells (**Figure 1**, inset). Wing cells are less flattened but have tight lateral junctions with their neighbors very similar to those observed in the squamous cells [2]. Finally, basal cells constitute the deepest cell layer of the corneal epithelium (**Figure 1**, inset). This layer, around 20 µm thick, constitutes a single layer of columnar epithelial cells that are connected through gap junctions and desmosomes and are attached to the underlying basement membrane by hemidesmosomes, preventing the epithelium from separating from the other corneal layers [2].

In mice, the epithelium contributes approximately 30% to the total corneal thickness. The stratified layout of the murine corneal epithelium is consistent with the description of this epithelium in the mammalian cornea. However, the mouse corneal epithelium consists of approximately twice the layers of cells compared with the human epithelium, with a higher number of squamous cells [15].

Corneal epithelial cell layers turn over every 7–10 days [16] following a delicate balance between superficial cell shedding and cell proliferation and migration from basal cells. Basal progenitor epithelial cells from the limbus (limbal stem cells) migrate towards the center of the cornea where they differentiate into transient amplifying cells (TA). TA basal cells, which are two horizontal progenies from the stem cells, migrate from the limbus to the periphery of the cornea to reach the center and undergo mixed proliferation (one daughter cell is retained in the basal cell layer, and the other moves into the middle layers of the epithelium). Once TA cells reach the end of their proliferative capacity, they become basal epithelial cells. Basal epithelial cells undergo vertical proliferation in two daughter cells resulting in two wing cells and eventually into two squamous cells that will be later shed by blinking. This concept was coined the X, Y, Z hypothesis of Thoft and Friend [17] where X is the basal corneal epithelial cell horizontal migration and vertical terminal proliferation, Y is the limbal cell proliferation and migration and Z is the squamous corneal epithelial cell shedding.

Between the corneal epithelium and the next corneal layer, the stroma, there is the epithelial basement membrane synthesized by epithelium basal cells. This membrane, also called the basal lamina, is approximately 0.05 µm thick and comprises laminin, type IV collagen, heparan sulfate, and fibronectin. Basal lamina serves as a scaffold for epithelial cell movement and attachment, and it is composed of two distinct layers when observed by electron microscopy: the more external *Lamina lucida* and a thicker more internal *Lamina densa* [1].

2.2. Bowman's Layer

Bowman’s layer in the human cornea is an acellular condensate of collagen types IV, V, VI, and VII arranged randomly [3] that help the cornea to maintain its shape [2]. This layer is approximately 15 µm thick and is associated with the basal lamina of the epithelium and continues with the stroma. Different roles have been ascribed to this layer of the cornea that is not present in all species, such as that it provides some kind of barrier function against the passage of macromolecules, such as medium and large size proteins, or that it is responsible for a substantial portion of the biomechanical rigidity of the cornea. However, there are also studies that conclude the opposite and the exact function of this layer remains unclear (see Wilson 2020 for a review [18]). It has been hypothesized that Bowman’s layer develops because of cytokine-mediated interactions occurring between corneal epithelial cells and the underlying keratocytes, including negative

chemotactic and apoptotic effects on the keratocytes by low levels of cytokines, such as interleukin-1α [19]. Bowman's layer is highly resistant to damage, but it cannot regenerate after injury and may result in a scar [20].

It is worth mentioning that in mice, subepithelial collagen fibers are also arranged randomly forming what would be a thin Bowman's layer. However, some authors believe that this is not a true layer [21] but an adaptation of the stromal tissue [15].

2.3. Stroma

Corneal stroma comprises 90% of the total corneal thickness [1]. It is mainly composed of water (78%), an organized structural network of types I and V collagen fibers (80% of corneal stroma's dry weight), keratocytes, and extracellular matrix.

The stromal collagen fibers are arranged in parallel bundles (fibrils) that are packed in parallel arranged layers (lamellae). In turn, each of these layers is arranged at right angles relative to fibers in adjacent lamellae, and this precise organization results in stromal transparency as it reduces forward light scatter [22].

Keratocytes, the major cell type of corneal stroma, are sandwiched between collagenous lamellae, mostly in the anterior stroma. These stellate-shaped cells are connected to each other through gap junctions present on their numerous dendritic processes [23]. Keratocytes are involved in maintaining the extracellular matrix environment and stromal composition as they are able to synthesize glycosaminoglycans, collagen molecules, and matrix metalloproteases (MMPs) [2]. As a first response to stromal injury, keratocytes are activated and migrate taking on a fibroblast-like appearance [24] and within 1–2 weeks of the initial insult, myofibroblasts enter the injured area and become involved in the stromal remodeling which can take months or even years to complete [2].

In mice, the corneal stroma accounts for two-thirds of the total corneal thickness. In these animals, stromal collagen fibers have a diameter of 29 ± 4 nm [25] with keratocytes arranged parallel to the collagen bundles.

In the posterior part of the human corneal stroma, there is a distinct region that constitutes the separation between the stroma and the Descemet's membrane. This pre-Descemet or Dua's layer is acellular and composed of 5 to 8 lamellae of predominantly type-1 collagen bundles arranged in transverse, longitudinal, and oblique directions [26].

2.4. Descemet's Membrane

Descemet's membrane is primarily composed of types IV and VIII collagen fibrils as well as the glycoproteins fibronectin, laminin, and thrombospondin. It is less strong and stiff than the posterior stroma and is secreted by endothelial cells since the 8th gestation week [2]. Descemet's membrane has a thickening rate of approximately 1 µm per decade of life: its thickness is around 4 µm at birth, while at the end of the normal lifespan Descemet's membrane is around 10–15 µm thick [1]. In addition, this thickness can also increase focally or diffusely with injury (trauma or surgery) or disease, due to abnormal collagen deposition.

Descemet's membrane in mice is more homogeneous and granular on the anterior chamber side, resembling a typical basal lamina, and it also becomes thicker with age [27].

2.5. Endothelium

The corneal endothelium is a monolayer of hexagonal cells whose density and topography change continuously throughout life [2]. At birth, corneal endothelium is 10 µm thick and its cell density is approximately 3500 cells/mm^2, however, this number decreases at approximately 0.6% per year [2]. Corneal endothelium maintains its continuity by migration and expansion of survival cells to cover the defect surface, so the percentage of hexagonal cells decreases (*pleomorphism*, that is, endothelial cells become different from each other in shape), while the coefficient of variation in cell area increases (*polymegathism*, that is, endothelial cells become different from each other in size, appearing large cells) [1].

The main function of the corneal endothelium is to maintain corneal transparency and health by regulating its hydration and nutrition [1]. Adjacent endothelial cells share extensive lateral interdigitations and possess tight and gap junctions along their apical and lateral borders, respectively, forming an incomplete barrier with a preference for the diffusion of small molecules [1]. The endothelium acts as a "leaky" barrier that allows passive fluid flow from the hypotonic corneal stroma to hypertonic aqueous humor through the osmotic gradient, maintaining the relatively dehydrated state of the stroma. Nevertheless, although this passive movement does not require energy, endothelial cells maintain the osmotic

gradient by active transport of ions. In this context, the major transport protein found to be essential is Na^+/K^+-ATPase, present in the basolateral membranes of endothelial cells.

3. Corneal Innervation

The cornea is supplied by both sensory and autonomic nerves, being one of the most densely innervated tissues in the body [5]. The trigeminal nerve, the major sensory nerve of the head, has three different sensory branches: ophthalmic (V1), maxillary (V2), and mandibular (V3) [28][29]. Most nerves supplying the cornea are sensory nerves, and most of them have their origin in the ophthalmic branch of the trigeminal ganglion (TG). Furthermore, a little innervation from the maxillary branch has also been reported in the inferior cornea and the conjunctiva [30][31].

V1 branches into the frontal, the lachrymal, and the nasociliary nerves. In turn, the nasociliary nerve branches into two long ciliary nerves and a connecting branch with the ciliary ganglion, a parasympathetic ganglion that sends 5–10 short ciliary nerves carrying both trigeminal sensory nerve fibers from the nasociliary nerve and parasympathetic and sympathetic axons, the last from the superior cervical ganglion. The density of the sympathetic nerves varies significantly among different species [32], being higher in the cat and rabbit cornea [33][34][35] and very sparse in humans and other primates [33][36].

Short and long ciliary nerves enter the posterior globe medially and laterally to the optic nerve [29][37], penetrating the sclera. After that, they form a ring around the optic nerve and travel anteriorly in the suprachoroidal space towards the anterior segment of the eye [29], undergoing repetitive branching. When reaching the limbal area, some fibers innervate the ciliary body and the iris, while most fibers form a dense ring-like network that encircles the limbus around the cornea, giving rise to the limbal plexus [38]. The majority of nerve fibers in this plexus are believed to be vasomotor nerves innervating limbal blood vessels, while a variable number of nerve trunks enter the corneal stroma unrelated to blood vessels [39].

3.1. Corneal Nerve Architecture

The architecture of corneal innervation has been studied for many years by a wide variety of methods, including light and electron microscopy, immunohistochemistry, and IVCM, among others. Moreover, it has been described among different species such as human [5][37], cat [35][40], guinea pig [41][42], and mouse [43][44]. Corneal innervation is anatomically organized into four levels from the penetrating stromal nerve trunks to the nerve terminals in the epithelium.

3.1.1. Stromal Nerves

Corneal stromal nerves enter the cornea radially through the corneoscleral limbus in the middle third of the stroma. In addition, other small nerve bundles enter the cornea more superficially in the episcleral and conjunctival planes, innervating the superficial stroma and the periphery of the corneal epithelium, respectively [38][40][41].

When entering the stroma at a depth of approximately 293 µm, myelinated axons (about 20%) lose their perineurium and myelin sheath [5] and run within the stroma as fascicles enclosed by a basal lamina and Remak Schwann cells (the non-myelinating Schwann cells) [29]. The distal branches of this arborization anastomose extensively form the anterior stromal nerve plexus, a complex network of nerve bundles and individual axons. The posterior half of the stroma and endothelium, on the contrary, are devoid of sensory nerve fibers [29].

In mice, stromal nerves do not enter the cornea radially at regular intervals as in humans. Stromal innervation is provided by nerve bundles entering into the cornea from four quadrants and branching irregularly to cover the entire cornea (**Figure 2**A,B).

In humans and higher mammals, the most superficial layer of the anterior stromal nerve plexus, immediately beneath Bowman's layer, is referred to as the corneal subepithelial nerve plexus. The subepithelial plexus has a very high nerve density, but in general, it is denser in the peripheral and intermediate cornea, and less dense in the central cornea [37].

Anatomically, in the subepithelial plexus, there are two distinct types of nerve bundles [29][38]. One form a complex anastomotic meshwork of single axons and thin tortuous fascicles that do not penetrate Bowman's membrane, while the second type consists of about 400–500 medium-sized, curvilinear bundles that turn 90° and penetrate Bowman's layer and basal lamina mainly in the peripheral and intermediate cornea [5][37]. These nerve bundles terminate in bulb-like structures and divide into smaller ones in groups up to 20 subbasal nerve fibers, known as epithelial leashes [5][37]. These leashes, which are parallel to the ocular surface, anastomose extensively to form a dense subbasal nerve plexus (see below).

It is worth mentioning that while unmyelinated nerves maintain their Remak Schwann cell coating in the stroma, they shed them before penetrating the basal lamina. In this regard, it has been suggested that corneal epithelial cells function as surrogate Schwann cells for the subbasal and intraepithelial nerves in healthy conditions and after injury [45].

3.1.2. Subbasal Nerve Plexus

The corneal epithelium receives sensory nerve fibers either from the subepithelial plexus or directly from the conjunctival nerves [38][39]. The subbasal nerve plexus constitutes epithelial leashes from subepithelial nerves that anastomose extensively and interconnect repeatedly with one another such that they are no longer recognizable as individual leashes (**Figure 2**C,D), although leashes are less numerous and separated in the periphery [37]. The term “epithelial leash” was defined as a group of subbasal nerves that derive from the same parent anterior stromal nerve trunk [40][46][47], being a unique neuroanatomical structure only found in the cornea of most species, including humans.

The subbasal nerve plexus is a dense, homogenous nerve plexus situated between the basal epithelial cells and the basal lamina. In humans, it is formed by 5000–7000 nerve fascicles in an area of about 90 mm^2 [48], with a total number of axons estimated to vary between 20,000 and 44,000 [5]. Morphologically, each leash consists of a variable number of straight nerve fibers, each containing 3–10 individual axons traveling up to several millimeters. Subbasal nerve fibers converge on a spiral whose center is called the vortex [49][50]. This vortex is also present in other species, including mice [42][43] and rats [51], and the mechanisms underlying its formation remain unclear. The most extended hypothesis is that nerves and basal epithelial cells advance in the same direction and velocity in a whorl-like pattern in response to chemotropic guidance, electromagnetic cues, and/or to population pressures [52][53].

3.1.3. Intraepithelial Nerve Terminals

Single nerve fibers arising from the subbasal plexus split off and turn 90° vertically as a profusion of terminal axons ascending between the epithelial cells, often with a modest amount of additional branching (**Figure 2**E–I) [29]. The term intraepithelial nerve terminal was defined by Carl Marfurt as the entire epithelial axon distal to its point of origin from a subbasal nerve and all its collateral branches and terminal expansions (the so-called nerve endings) [37]. Corneal epithelium innervation is extremely dense. It is estimated that the human central cornea contains around 5000–7000 nerve terminals per square millimeter, although this number changes throughout life and in ocular pathologies.

The intraepithelial nerve terminals innervate the corneal epithelium through all its layers. Those running between the basal and wing epithelium cells run in a horizontal direction and branch relatively infrequently [37], while intraepithelial nerve terminals that terminate within the more superficial cell layers are generally more complex (**Figure 2**E,G–I). Intraepithelial nerve terminals can be classified into three different types: simple, ramifying, and complex [28]. Simple terminals do not branch after leaving the subbasal plexus and end with a bulbar swelling within or below the superficial squamous cells [28][42] (**Figure 2**G). Simple terminals are more abundant in the central cornea. Ramifying terminals branch within the squamous cell layer into 3–4 branches that run horizontally for a hundred microns and that end in a single bulbar swelling like the simple terminals [28][42] (**Figure 2**H), being more numerous in the peripheral cornea [42]. Finally, axons forming the complex terminals start to branch within the wing cells layer and terminate with multiple larger bulbous endings within the wing and squamous cell layers (**Figure 2**I). Complex terminals are found in the central and the peripheral cornea, but their complexity and size are higher in the periphery [42].

Intraepithelial nerve terminals seem to be functionally different as immunocytochemical staining reveals differences in the expression of neuropeptides and neurotransmitters. In mice and guinea pigs, nerves that terminate in the basal epithelium and the outermost cell layers have simple endings immunopositive for Calcitonin Gene-Related Peptide (CGRP) and substance P (SP), suggesting that peptidergic simple nerve terminals correspond functionally to polymodal nociceptor nerve terminals [42]. On the other hand, complex nerve terminals are immunoreactive to TRPM8 (Transient receptor potential channel subfamily M member 8), supporting the idea that complex terminals correspond to cold thermoreceptor terminals [42]. More recent studies in guinea pig corneas also suggest that these intraepithelial nerve terminals can be distinguished morphologically as TRPM8-positive terminals are more complex than TRPV1-positive terminals [54].

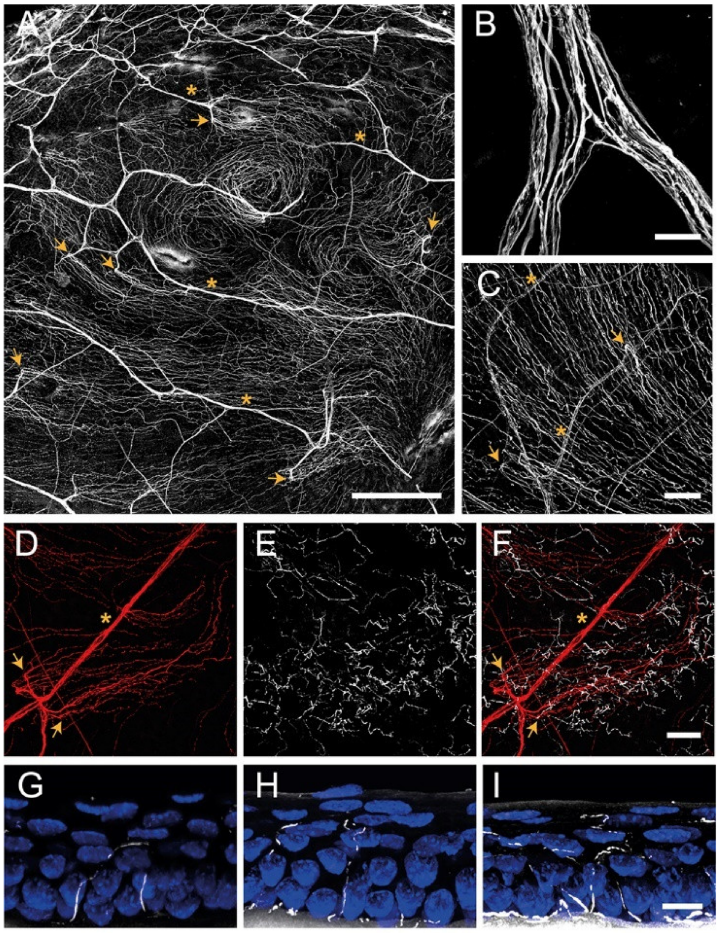

Figure 2. Confocal images of sensory nerves immunostained with anti–β tubulin III antibody in mouse cornea. (**A**) Sensory nerve trunks enter from the limbus into the stroma of the cornea where they ramify, giving rise to a dense subepithelial plexus (asterisks). (**B**) Detail of a stromal nerve trunk branching. (**C**,**D**) From the stroma, nerve fibers penetrate through the basal lamina (arrowheads) and form the subbasal plexus. Subbasal nerve fibers run parallel for a long distance within the epithelium basal cell layer. (**E**–**I**) Subbasal nerves give rise to terminal branches that ascend along their trajectory through the epithelial cells. According to the number of branches, three morphological types of corneal nerve terminals are identified: simple (**G**), ramified (**H**), and complex (**I**) nerve terminals. Scale bars: (**A**) 250 µm; (**B**) 25 µm; (**C**–**F**) 50 µm; (**G**–**I**) 10 µm. Methods: C57BL/6J eyes were fixed for 2 h at RT in methanol and DMSO (4:1), incubated 5 min at −20 °C in methanol, rehydrated, and washed in PBS. (**A**–**F**) Corneas were dissected, incubated 2 h at RT in blocking solution (5% goat normal serum, 1% BSA and 0.1%Triton X–100 in PBS) and 48 h at 4 °C with anti–β tubulin III antibody (1:500 in blocking solution; #801201, BioLegend, CA, San Diego, USA), rinsed and then incubated for 2 h at RT with AF555 (1:500 in PBS; #A32727, ThermoFisher Scientific, OR, Waltham, USA), washed in PBS and mounted with Fluoromount-G (ThermoFisher Scientific). (**G**–**I**) Eyes were cryoprotected (30% sucrose in PBS overnight at 4 °C), embedded in OCT, frozen in liquid nitrogen, cut on a cryostat in serial 15 mm thick sections, and mounted in slides. Tissue sections were rinsed in 0.03% Triton X–100 in PBS and then for 30 min in blocking solution followed by overnight incubation at 4 °C with anti–β tubulin III antibody in blocking solution, washing with PBS and incubation with AF555 in PBS for 2 h at RT. Afterward, slides were rinsed with PBS, incubated with Hoechst 33342 (10 µm/mL; #H1399, ThermoFisher Scientific), and coverslipped with Fluoromount–G. Images were collected using a laser scanning confocal microscope Zeiss LSM 880 (Oberkochen, DEU).

3.2. Functional Types of Corneal Nerves

Electrophysiological recordings of sensory nerve fibers innervating the cornea have revealed the existence of different functional types of ocular sensory nerves, classically classified depending on the modality of stimulus by which they are activated [6][55]. Most corneal sensory nerves are the peripheral branches of medium or small trigeminal neurons with thin myelinated (A-delta) or unmyelinated (C) axons [55]. The external stimuli are transduced by their intraepithelial nerve terminals into a discharge of nerve impulses that encode the stimulus' spatial and temporal characteristics. The impulse discharge is conducted by trigeminal neurons to the central nervous system, where sensory input is processed to finally evoke a sensation and is also used to regulate protective functions, such as tearing and blinking. Depending on the variable activation of the different classes of corneal sensory neurons, different sensations are evoked [6][56].

3.2.1. Mechanonociceptors

About 15% of corneal nerve fibers are mechanonociceptors, which express Piezo2 channels [57][58] and are activated exclusively by mechanical forces (**Figure 3**). Mechanonociceptors are usually A-delta fibers and produce a short-lasting impulse discharge in response to a sustained mechanical stimulus, therefore signaling the presence and velocity of change in the mechanical force, rather than its intensity or duration [59][60]. These relatively rapidly adapting mechanosensitive fibers contribute to the pain experienced when a foreign body touches the ocular surface [56].

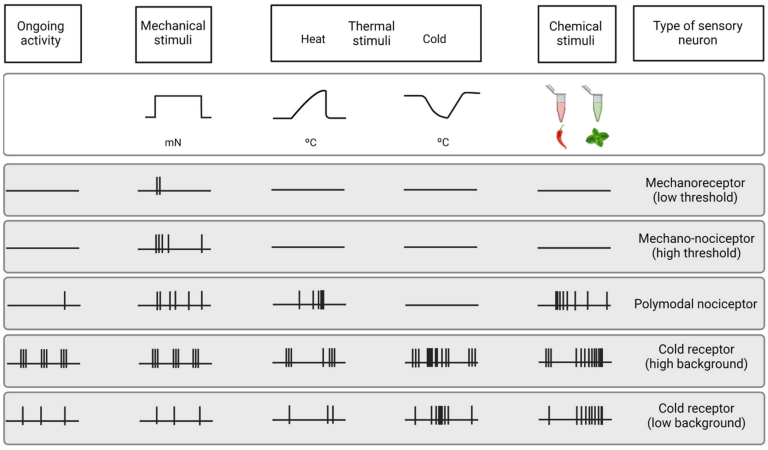

Figure 3. Functional types of sensory neurons innervating the cornea. Schematic representation of the spontaneous and stimulus-evoked nerve impulse activity of the different functional types of sensory nerves innervating the cornea. Based on the characteristics of the impulse discharge in absence of intended stimulation (ongoing activity) and response to different types of stimuli (upper part of the figure), the peripheral terminals of primary sensory neurons innervating the cornea are classified into five different functional types of sensory neurons.

3.2.2. Polymodal Nociceptors

The majority of corneal sensory fibers (around 70%) are polymodal nociceptors, which express a diversity of transducing ion channels in their nerve terminals, such as TRPA1,TRPV1, ASIC, and Piezo2, that allow them to be activated by noxious mechanical forces, heat (temperatures over 39ºC) and a wide variety of exogenous and endogenous chemicals (protons, ATP, prostaglandins, cytokines, etc.) [7][61] **(Figure 3)**. Polymodal nociceptors produce an irregular and repetitive discharge as long as thestimulus is maintained that is proportional to its intensity [7][62]. Moreover, under certain circumstances, polymodal nociceptors can be sensitized, developing an irregular low frequency long after the stimulus has disappeared [63]. In addition, sensitization produces a decrease in threshold and an increase in the firing frequency in response to a new stimulus [59][64]. Most corneal polymodal nociceptors are slow-conducting C-type fibers and are the origin of the ocular discomfort and pain sensations developed under pathological conditions, local inflammation, or injury [63][65].

3.2.3. Cold Thermoreceptors

The third class of corneal sensory fibers is cold thermoreceptors (10–15%), associated with A-delta and C nerve fibers. Cold thermoreceptors have spontaneous discharge and increase their firing rate in response to temperature reduction and osmolality increases [62][66][67] **(Figure 3)**. Cold thermoreceptors are transiently silenced upon warming, although some of them restart firing in response to high temperatures (paradoxical response to heat) [6][68]. Cold thermoreceptors firing increases proportionally to the speed and magnitude of the corneal temperature reduction, as well as to the final static temperature [6]. When enough cold thermoreceptors are recruited with augmented tear evaporation, a conscious sensation of dryness is expected [55]. Cooling sensations with temperature reductions are increasingly unpleasant when higher temperature decreases are applied [56].

The activity of corneal cold thermoreceptors expressing TRPM8 is crucial in different mechanisms protecting the eye, such as lacrimation and blinking [6][69][70][71]. The deletion of TRPM8 channels produces both a decrease in basal tearing [70] and blinking [71] in mice, supporting the idea that sensory input of cold thermoreceptors is used by the CNS to regulate blinking and tearing. Aging induces changes in TRPM8 expression and activity, which correlates with the changes in tearing developed with age [72].

3.3. Changes of Nerve Activity under Inflammation and after Injury

After inflammation or lesion, corneal sensory nerve activity is altered. Like in other tissues, corneal nociceptors (specially polymodal nociceptors) are sensitized [63][68][73][74][75][76][77][78], a functional state characterized by an increase in spontaneous activity, a reduction in the response threshold, and an increased response to stimulation. Sensitization

constitutes the basis of spontaneous pain and hyperalgesia experienced during inflammation. Additionally, corneal nociceptors also contribute to the inflammatory processes of the ocular surface (a process known as neurogenic inflammation) [79][80] by releasing pro-inflammatory neuropeptides, such as SP and CGRP [5][81][82]. After injury, regenerating nociceptors present increased spontaneous activity due to the increased expression of specific types of Na+channels by regenerating neurons [78]. Contrarily, cold thermoreceptors' activity is decreased under inflammation [68] [75] because the activity of TRPM8 channels is inhibited by inflammatory mediators, such as bradykinin through a G-protein [83]. During chronic tear deficiency, the activity of cold thermoreceptors is increased due to the increase in Na+ currents and the decrease in K+ currents [76].

References

1. Dawson, D.G.; Ubels, J.L.; Edelhauser, H.F. Cornea and sclera. In Adler's Physiology of the Eye, 11th ed.; Elsevier: Amsterdam, The Netherlands, 2011; Volume 4, pp. 71–130.
2. DelMonte, D.W.; Kim, T. Anatomy and physiology of the cornea. J. Cataract Refract. Surg. 2011, 37, 588–598.
3. Saude, T. Ocular Anatomy and Physiology; Blackwell Science Ltd.: Oxford, UK, 1993.
4. Rüfer, F.; Schröder, A.; Erb, C. White-to-white corneal diameter: Normal values in healthy humans obtained with the Orbscan II topography system. Cornea 2005, 24, 259–261.
5. Müller, L.J.; Marfurt, C.F.; Kruse, F.; Tervo, T.M.T. Corneal nerves: Structure, contents and function. Exp. Eye Res. 2003, 76, 521–542.
6. Belmonte, C.; Gallar, J. Cold thermoreceptors, unexpected players in tear production and ocular dryness sensations. Investig. Ophthalmol. Vis. Sci. 2011, 52, 3888–3892.
7. Belmonte, C.; Aracil, A.; Acosta, M.C.; Luna, C.; Gallar, J. Nerves and sensations from the eye surface. Ocul. Surf. 2004, 2, 248–253.
8. González-González, O.; Bech, F.; Gallar, J.; Merayo-Lloves, J.; Belmonte, C. Functional properties of sensory nerve terminals of the mouse cornea. Investig. Ophthalmol. Vis. Sci. 2017, 58, 404–415.
9. Maurice, D.M. The structure and transparency of the cornea. J. Physiol. 1957, 136, 263–286.
10. Hassell, J.R.; Birk, D.E. The molecular basis of corneal transparency. Exp. Eye Res. 2010, 91, 326–335.
11. Ambati, B.K.; Nozaki, M.; Singh, N.; Takeda, A.; Jani, P.D.; Suthar, T.; Albuquerque, R.J.C.; Richter, E.; Sakurai, E.; Newcomb, M.T.; et al. Corneal avascularity is due to soluble VEGF receptor-1. Nature 2006, 443, 993–997.
12. Cursiefen, C.; Chen, L.; Saint-Geniez, M.; Hamrah, P.; Jin, Y.; Rashid, S.; Pytowski, B.; Persaud, K.; Wu, Y.; Streilein, J.W.; et al. Nonvascular VEGF receptor 3 expression by corneal epithelium maintains avascularity and vision. Proc. Natl. Acad. Sci. USA 2006, 103, 11405–11410.
13. Almubrad, T.; Akhtar, S. Structure of corneal layers, collagen fibrils, and proteoglycans of tree shrew cornea. Mol. Vis. 2011, 17, 2283–2291.
14. Argüeso, P.; Gipson, I.K. Epithelial mucins of the ocular surface: Structure, biosynthesis and function. Exp. Eye Res. 2001, 73, 281–289.
15. Henriksson, J.T.; McDermott, A.M.; Bergmanson, J.P.G. Dimensions and morphology of the cornea in three strains of mice. Investig. Ophthalmol. Vis. Sci. 2009, 50, 3648–3654.
16. Hanna, C.; Bicknell, D.S.; O'brien, J.E. Cell Turnover in the Adult Human Eye. Arch. Ophthalmol. 1961, 65, 695–698.
17. Thoft, R.A.; Friend, J. The X, Y, Z hypothesis of corneal epithelial maintenance. Investig. Ophthalmol. Vis. Sci. 1983, 24, 1442–1443.
18. Wilson, S.E. Bowman's layer in the cornea– structure and function and regeneration. Exp. Eye Res. 2020, 195, 108033.
19. Wilson, S.E.; Hong, J.W. Bowman's layer structure and function: Critical or dispensable to corneal function? A Hypothesis. Cornea 2000, 19, 417–420.
20. Lee, T. The ins and outs of corneal wound healing. Rev. Optom. 2016, 153, 44–56.
21. Hazlett, L.D. Corneal and Ocular Surface Histochemistry. Prog. Histochem. Cytochem. 1993, 25, 3–6.
22. Maurice, D.M. The transparency of the corneal stroma. Vision Res. 1970, 10, 107–108.
23. Watsky, M.A. Keratocyte gap junctional communication in normal and wounded rabbit corneas and human corneas. Investig. Ophthalmol. Vis. Sci. 1995, 36, 2568–2576.

24. Stramer, B.M.; Zieske, J.D.; Jung, J.C.; Austin, J.S.; Fini, M.E. Molecular mechanisms controlling the fibrotic repair phenotype in cornea: Implications for surgical outcomes. Investig. Ophthalmol. Vis. Sci. 2003, 44, 4237–4246.
25. Haustein, J. On the ultrastructure of the developing and adult mouse corneal stroma. Anat. Embryol. 1983, 168, 291–305.
26. Dua, H.S.; Faraj, L.A.; Said, D.G.; Gray, T.; Lowe, J. Human corneal anatomy redefined: A novel pre-Descemet's layer (Dua's layer). Ophthalmology 2013, 120, 1778–1785.
27. Smith, R.S.; Sundberg, J.P.; John., S.W.M. The anterior segment and ocular adnexae. In Systematic Evaluation of the Mouse Eye: Anatomy, Pathology and Biomethods; Smith, R.S., Ed.; CRC Press: Boca Raton, FL, USA, 2002; Volume 1, pp. 3–23.
28. Al-Aqaba, M.A.; Dhillon, V.K.; Mohammed, I.; Said, D.G.; Dua, H.S. Corneal nerves in health and disease. Prog. Retin. Eye Res. 2019, 73, 100762.
29. Belmonte, C.; Tervo, T.T.; Gallar, J. Sensory innervation of the eye. In Adler's Physiology of the Eye, 11th ed.; Elsevier: Amsterdam, The Netherlands, 2011; Volume 16, pp. 363–384.
30. Vonderahe, A.R. Corneal and scleral anesthesia of the lower hale of the eye in a case of trauma of the superior maxillary nerve. Arch. Neurol. Psychiatry 1928, 20, 836–837.
31. Ruskell, G.L. Ocular fibers of the maxillary nerve in monkeys. J. Anat. 1974, 118, 195–203.
32. Marfurt, C.F.; Ellis, L.C. Immunohistochemical localization of tyrosine hydroxylase in corneal nerves. J. Comp. Neurol. 1993, 336, 517–531.
33. Ehinger, B. Connections between Adrenergic Nerves and other Tissue Components in the Eye. Acta Physiol. Scand. 1966, 67, 57–64.
34. Morgan, C.; DeGroat, W.C.; Jannetta, P.J. Sympathetic innervation of the cornea from the superior cervical ganglion. An HRP study in the cat. J. Auton. Nerv. Syst. 1987, 20, 179–183.
35. Marfurt, C.F.; Kingsley, R.E.; Echtenkamp, S.E. Sensory and sympathetic innervation of the mammalian cornea. A retrograde tracing study. Investig. Ophthalmol. Vis. Sci. 1989, 30, 461–472.
36. Toivanen, M.; Tervo, T.; Partanen, M.; Vannas, A.; Hervonen, A. Histochemical demonstration of adrenergic nerves in the stroma of human cornea. Investig. Ophthalmol. Vis. Sci. 1987, 28, 398–400.
37. Marfurt, C.F.; Cox, J.; Deek, S.; Dvorscak, L. Anatomy of the human corneal innervation. Exp. Eye Res. 2010, 90, 478–492.
38. He, J.; Bazan, N.G.; Bazan, H.E.P. Mapping the entire human corneal nerve architecture. Exp. Eye Res. 2010, 91, 513–523.
39. Marfurt, C.F. Nervous control of the cornea. In Nervous Control of the Eye; Harwood Academic Publishers: Amsterdam, The Netherlands, 2000; p. 41.
40. Chan-Ling, T. Sensitivity and neural organization of the cat cornea. Investig. Ophthalmol. Vis. Sci. 1989, 30, 1075–1082.
41. Zander, E.; Weddell, G. Observations on the innervation of the cornea. J. Anat. 1951, 85, 68–99.
42. Ivanusic, J.J.; Wood, R.J.; Brock, J.A. Sensory and sympathetic innervation of the mouse and guinea pig corneal epithelium. J. Comp. Neurol. 2013, 521, 877–893.
43. Mckenna, C.C.; Lwigale, P.Y. Innervation of the mouse cornea during development. Investig. Ophthalmol. Vis. Sci. 2011, 52, 30–35.
44. Wang, C.; Fu, T.; Xia, C.; Li, Z. Changes in mouse corneal epithelial innervation with age. Investig. Ophthalmol. Vis. Sci. 2012, 53, 5077–5084.
45. Stepp, M.A.; Tadvalkar, G.; Hakh, R.; Pal-Ghosh, S. Corneal epithelial cells function as surrogate Schwann cells for their sensory nerves. Glia 2017, 65, 851–863.
46. Rózsa, A.J.; Beuerman, R.W. Density and organization of free nerve endings in the corneal epithelium of the rabbit. Pain 1982, 14, 105–120.
47. Schimmelpfennig, B. Nerve structures in human central corneal epithelium. Graefe's Arch. Clin. Exp. Ophthalmol. 1982, 218, 14–20.
48. Belmonte, C.; Garcia-Hirschfeld, J.; Gallar, J. Neurobiology of ocular pain. Progr. Ret. Eye Res. 1997, 16, 117–156.
49. Dua, H.S.; Watson, N.J.; Mathur, R.M.; Forrester, J.V. Corneal epithelial cell migration in humans: 'hurricane and blizzard keratopathy'. Eye 1993, 7, 53–58.

50. Al-Aqaba, M.A.; Fares, U.; Suleman, H.; Lowe, J.; Dua, H.S. Architecture and distribution of human corneal nerves. Br. J. Ophthalmol. 2010, 94, 784–789.

51. Dvorscak, L.; Marfurt, C.F. Age-related changes in rat corneal epithelial nerve density. Investig. Ophthalmol. Vis. Sci. 2008, 49, 910–916.

52. Nagasaki, T.; Zhao, J. Centripetal Movement of Corneal Epithelial Cells in the Normal Adult Mouse. Investig. Ophthalmol. Vis. Sci. 2003, 44, 558–566.

53. Patel, D.V.; McGhee, C.N.J. Mapping of the normal human corneal sub-basal nerve plexus by in vivo laser scanning confocal microscopy. Investig. Ophthalmol. Vis. Sci. 2005, 46, 4485–4488.

54. Alamri, A.S.; Wood, R.J.; Ivanusic, J.J.; Brock, J.A. The neurochemistry and morphology of functionally identified corneal polymodal nociceptors and cold thermoreceptors. PLoS ONE 2018, 13, e0195108.

55. Belmonte, C.; Acosta, M.C.; Gallar, J. Neural basis of sensation in intact and injured corneas. Exp. Eye Res. 2004, 78, 513–525.

56. Acosta, M.C.; Belmonte, C.; Gallar, J. Sensory experiences in humans and single-unit activity in cats evoked by polymodal stimulation of the cornea. J. Physiol. 2001, 534, 511–525.

57. Bron, R.; Wood, R.J.; Brock, J.A.; Ivanusic, J.J. Piezo2 expression in corneal afferent neurons. J. Comp. Neurol. 2014, 522, 2967–2979.

58. Fernández-Trillo, J.; Florez-Paz, D.; Íñigo-Portugués, A.; González-González, O.; del Campo, A.G.; González, A.; Viana, F.; Belmonte, C.; Gomis, A. Piezo2 mediates low-threshold mechanically evoked pain in the cornea. J. Neurosci. 2020, 40, 8976–8993.

59. Belmonte, C.; Giraldez, F. Responses of cat corneal sensory receptors to mechanical and thermal stimulation. J. Physiol. 1981, 321, 355–368.

60. Belmonte, C.; Gallar, J.; Pozo, M.A.; Rebollo, I. Excitation by irritant chemical substances of sensory afferent units in the cat's cornea. J. Physiol. 1991, 437, 709–725.

61. Belmonte, C.; Gallar, J.; Pozo, M.A.; Rebollo, I. Excitation by irritant chemical substances of sensory afferent units in the cat's cornea. J. Physiol. 1991, 437, 709–725.

62. Chen, X.; Gallar, J.; Belmonte, C. Reduction by antiinflammatory drugs of the response of corneal sensory nerve fibers to chemical irritation. Investig. Ophthalmol. Vis. Sci. 1997, 38, 1944–1953.

63. Gallar, J.; Pozo, M.A.; Tuckett, R.P.; Belmonte, C. Response of sensory units with unmyelinated fibres to mechanical, thermal and chemical stimulation of the cat's cornea. J. Physiol. 1993, 468, 609–622.

64. Gallar, J.; Acosta, M.C.; Gutiérrez, A.R.; Belmonte, C. Impulse activity in corneal sensory nerve fibers after photorefractive keratectomy. Investig. Ophthalmol. Vis. Sci. 2007, 48, 4033–4037.

65. Bessou, P.; Perl, E.R. Response of cutaneous sensory units with unmyelinated fibers to noxious stimuli. J. Neurophysiol. 1969, 32, 1025–1043.

66. Meyer, R.A.; Ringkamp, M.; Campbell, J.N.; Raja, S.N. Peripheral mechanisms of cutaneous nociception. In Wall & Melzack's Textbook of Pain; Elsevier: Amsterdam, The Netherlands, 2006; pp. 3–34.

67. Carr, R.W.; Pianova, S.; Fernandez, J.; Fallon, J.B.; Belmonte, C.; Brock, J.A. Effects of heating and cooling on nerve terminal impulses recorded from cold-sensitive receptors in the guinea-pig cornea. J. Gen. Physiol. 2003, 121, 427–439.

68. Parra, A.; Gonzalez-Gonzalez, O.; Gallar, J.; Belmonte, C. Tear fluid hyperosmolality increases nerve impulse activity of cold thermoreceptor endings of the cornea. Pain 2014, 155, 1481–1491.

69. Acosta, M.C.; Luna, C.; Quirce, S.; Belmonte, C.; Gallar, J. Changes in sensory activity of ocular surface sensory nerves during allergic keratoconjunctivitis. Pain 2013, 154, 2353–2362.

70. Acosta, M.C.; Peral, A.; Luna, C.; Pintor, J.; Belmonte, C.; Gallar, J. Tear secretion induced by selective stimulation of corneal and conjunctival sensory nerve fibers. Investig. Ophthalmol. Vis. Sci. 2004, 45, 2333–2336.

71. Parra, A.; Madrid, R.; Echevarria, D.; del Olmo, S.; Morenilla-Palao, C.; Acosta, M.C.; Gallar, J.; Dhaka, A.; Viana, F.; Belmonte, C. Ocular surface wetness is regulated by TRPM8-dependent cold thermoreceptors of the cornea. Nat. Med. 2010, 16, 1396–1399.

72. Quallo, T.; Vastani, N.; Horridge, E.; Gentry, C.; Parra, A.; Moss, S.; Viana, F.; Belmonte, C.; Andersson, D.A.; Bevan, S. TRPM8 is a neuronal osmosensor that regulates eye blinking in mice. Nat. Commun. 2015, 6, 7150.

73. Alcalde, I.; Íñigo-Portugués, A.; González-González, O.; Almaraz, L.; Artime, E.; Morenilla-Palao, C.; Gallar, J.; Viana, F.; Merayo-Lloves, J.; Belmonte, C. Morphological and functional changes in TRPM8-expressing corneal cold

thermoreceptor neurons during aging and their impact on tearing in mice. J. Comp. Neurol. 2018, 526, 1859–1874.

74. Gallar, J.; Acosta, M.C.; Moilanen, J.A.O.; Holopainen, J.M.; Belmonte, C.; Tervo, T.M.T. Recovery of corneal sensitivity to mechanical and chemical stimulation after laser in situ keratomileusis. J. Refract. Surg. 2004, 20, 229–235.
75. Luna, C.; Quirce, S.; Aracil-Marco, A.; Belmonte, C.; Gallar, J.; Acosta, M.C. Unilateral Corneal Insult Also Alters Sensory Nerve Activity in the Contralateral Eye. Front. Med. 2021, 8, 2079.
76. Acosta, M.C.; Luna, C.; Quirce, S.; Belmonte, C.; Gallar, J. Corneal sensory nerve activity in an experimental model of UV keratitis. Investig. Ophthalmol. Vis. Sci. 2014, 55, 3403–3412.
77. Kovács, I.; Luna, C.; Quirce, S.; Mizerska, K.; Callejo, G.; Riestra, A.; Fernández-Sánchez, L.; Meseguer, V.M.; Cuenca, N.; Merayo-Lloves, J.; et al. Abnormal activity of corneal cold thermoreceptors underlies the unpleasant sensations in dry eye disease. Pain 2016, 157, 399–417.
78. Belmonte, C. Pain, Dryness, and Itch Sensations in Eye Surface Disorders Are Defined by a Balance between Inflammation and Sensory Nerve Injury. Cornea 2019, 38, S11–S24.
79. Luna, C.; Mizerska, K.; Quirce, S.; Belmonte, C.; Gallar, J.; del Carmen Acosta, M.; Meseguer, V. Sodium Channel Blockers Modulate Abnormal Activity of Regenerating Nociceptive Corneal Nerves After Surgical Lesion. Investig. Opthalmol. Vis. Sci. 2021, 62, 2.
80. Gonzalez, G.G.; De la Rubia, P.G.; Gallar, J.; Belmonte, C. Reduction of capsaicin-induced ocular pain and neurogenic inflammation by calcium antagonists. Investig. Ophthalmol. Vis. Sci. 1993, 34, 3329–3335.
81. Vitar, R.M.L.; Barbariga, M.; Fonteyne, P.; Bignami, F.; Rama, P.; Ferrari, G. Modulating ocular surface pain through neurokinin-1 receptor blockade. Investig. Ophthalmol. Vis. Sci. 2021, 62, 26.
82. Murata, Y.; Masuko, S. Peripheral and central distribution of TRPV1, substance P and CGRP of rat corneal neurons. Brain Res. 2006, 1085, 87–94.
83. Yang, L.; Mehta, J.; Liu, Y.C. Corneal neuromediator profiles following laser refractive surgery. Neural Regen. Res. 2021, 16, 2177–2183.

Retrieved from https://encyclopedia.pub/entry/history/show/49845